Dual-stage nanofiltration seawater desalination: water quality, scaling and energy consumption

Jie Liu[a], Lixin Xie[b,c,]*, Zhi Wang[b,c,d], Junsheng Yuan[a]

[a]*Engineering Research Center of Seawater Utilization Technology of Ministry of Education, Hebei University of Technology, Box 307, No. 8, Guangrong Road, Tianjin 300130, P.R. China*
[b]*Chemical Engineering Research Center, School of Chemical Engineering and Technology, Tianjin University, No. 92, Weijin Road, Tianjin 300072, P.R. China*
Tel. +86 022 27404347; Fax: +86 022 87891367; email: xie_lixin@tju.edu.cn
[c]*Tianjin Key Laboratory of Membrane Science and Desalination Technology, Tianjin University, No. 92, Weijin Road, Tianjin 300072, P.R. China*
[d]*State Key Laboratory of Chemical Engineering, Tianjin University, Tianjin 300072, P.R. China*

ABSTRACT

A dual-stage nanofiltration (NF) seawater desalination process was investigated as a novel seawater desalination technology, focusing not only on the permeate water quality, but also on the scaling possibility and energy consumption. Dow Filmtec[TM] NF90 was used in the experiment for its high rejection of total dissolved solids (TDS). The results show that the permeate TDS from the second stage could be as low as 200 mg/L under an optimized condition. The operating pressures were only 3.5 MPa in the first stage and 2.0 MPa in the second stage. Operation pressure had the most significant effects on water permeate flux and TDS. Several indices were calculated to investigate scaling probability. The results indicate that scaling could occur in the first stage. Thus, a prevention method would be needed. The effects of the operating parameters on the energy consumption were also examined. The results indicate that dual-stage NF seawater desalination is a feasible technology in the view of water quality and energy consumption.

Keywords: Dual-stage nanofiltration (NF); Seawater desalination; Scaling; Energy consumption

1. Introduction

Seawater desalination has become an important new source of fresh water. Until 2009, the global installed desalination capacity had been more than $6 \times 10^7 \, m^3/d$, of which 60% was contributed by the seawater desalination processes. This figure is expected to increase in the future because of global water scarcity and technological development. The most common seawater desalination technologies currently used are reverse osmosis (RO), multi-stage flash (MSF) distillation, and multi-effect distillation (MED) [1], all of which are considered as the most reliable technologies, and have thus been extensively used commercially. Given the development of more efficient membrane elements and the use of energy recovery devices, the energy consumption of RO has been reduced to a value between 2.2 and 2.5 kWh/m³. RO is currently regarded as the most energy-saving

*Corresponding author.

desalination method [2,3]. MED and MSF are widely used in situations where sufficient thermal energy could be supplied. RO accounted for 60% of the global seawater desalination capacity, whereas the proportion of MED and MSF were only 8 and 26.8%, until 2009 [4]. Aside from these methods, several novel, alternative seawater desalination technologies, such as solar desalination [5,6], humidification–dehumidification [7] and so on [8–11], have been developed to meet different needs.

Nanofiltration (NF) is another promising technology in seawater desalination process. NF membrane has a molecular weight cut-off (MWCO) of 200–2,000 Dalton (Da), and it also has the separation characteristics to remove divalent ions (the ions prone to scaling) effectively. Much research work has been carried out on the utilization of NF membrane for seawater softening, and the results show that both the divalent ions and total dissolved solids (TDS) could be reduced [12–15]. At the same time, given its membrane structure, the water permeability level of NF membrane is higher than that of RO membrane. The operating pressure of an NF membrane is typically lower than 4 MPa; therefore, the energy consumption is also thought to be low. A number of special NF membranes with high TDS rejection also have been developed and commercially applied. All of these make the application of NF in seawater desalination possible, which is a new application of NF. Two-stage NF membranes with high TDS rejection level are utilized in a dual-stage NF seawater desalination process. Harrison et al. [16] carried out a bench-scale study using flat-sheet membrane cells to test the possibility of using NF membrane in seawater desalination. A series of basic data were obtained, including mass-transfer coefficients, ion rejection and water flux. NF90 and NE90 were found to be suitable for the seawater desalination process. Chen et al. [17] performed a single-element membrane test for dual-stage NF seawater desalination in which four different membranes were compared. The TDS of permeates from second stage was 218 mg/L, lower than that of Long Beach tap water (390 mg/L). Al Taee and Sharif [18] proposed an NF–BWRO dual-stage desalination process similar to the dual-stage NF desalination process and investigated its applicability and cost-effectiveness by using the ROSA[TM] software. The simulation results showed that the overall cost of NF–NF was slightly lower than that of the NF–BWRO process; however, this was at the cost of higher permeate TDS.

These mentioned researches have been carried out to prove the feasibility of dual-stage NF seawater desalination. However, certain key aspects have not been investigated, such as the influence of operating conditions on scaling possibility and energy consumption in both stages. These factors are significant in the application of dual-stage NF seawater desalination technology. Thus, the present study focuses on the effects of operating factors on the rejection of ions and TDS, as well as on the system recovery. More importantly, scaling possibility and energy consumption are examined in detail to investigate potential industrial applications of dual-stage NF seawater desalination.

2. Experimental and materials

2.1. Experimental

The experiments were conducted with single-element equipment, as shown in the diagram in Fig. 1. Artificial seawater was prepared as raw water and was pumped into the NF membrane. The flow rate and pressure of the feed water could be adjusted by the pump and a retentate stream valve. Both permeate and retentate were supplied back to the raw water vessel to assure that the concentration would remain constant. The sample was taken 30 min later, after the flow rate and the pressure were set. Optimized operating conditions were selected in the first stage of experiment, the permeate water of which was used as feed water in the second-stage experiment.

2.2. Materials

The composition of the artificial seawater is listed in Table 1. The NF membrane used in the experiments was Filmtec[TM] NF90-4040 of DOW Co. Ltd., and its properties are presented in Table 2.

2.3. Analysis

The concentrations of Ca^{2+} and Mg^{2+} were analyzed via ethylenediaminetetraacetic (EDTA) titration methods. The concentration of Cl^- was determined by
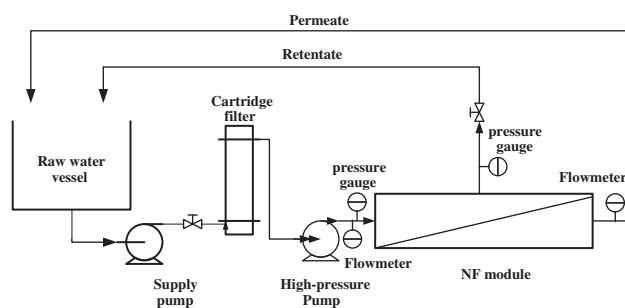

Fig. 1. Diagram of the experimental equipment.

Table 1
Ion concentration in the artificial seawater

Ion	Concentration (mg/L)
SO_4^{2-}	2,710
Cl^-	19,350
Ca^{2+}	410
Mg^{2+}	1,290
Na^+	10,770
HCO_3^-	140
TDS	34,670

Fig. 2. Influence of feed pressure on ions rejection ratio ($24°C$, $1.8\,m^3/h$).

Table 2
Performance of NF90-4040

Model	Membrane area (m^2)	Permeate water flux (L/h)	TDS rejection (%)	Max operating pressure (MPa)
NF90-4040	7.6	291.7	>97	4.1

Test conditions: 2,000 mg/L $MgSO_4$, 0.48 MPa, 25°C, and recovery ratio 15%.

means of "Silver Nitrate Titration" (ASTM D512-89 (1999) "Standard Test Methods for Chloride Ion In Water"), whereas the HCO_3^- was titrated by an HCl solution. The concentration of SO_4^{2-} was examined through the use of a DR2800 Hach® spectrophotometer, and the concentration of Na^+ was calculated by the charge balance as follows:

$$C_{Na^+} = \left(\left(\frac{C_{SO_4^{2-}}}{96} \right) \times 2 + \frac{C_{HCO_3^-}}{61} + \frac{C_{Cl^-}}{35.5} - \left(\frac{C_{Ca^{2+}}}{40} \right) \times 2 \right.$$
$$\left. - \left(\frac{C_{Mg^{2+}}}{24} \right) \times 2 \right) \times 23 \tag{1}$$

where C is the ion concentration.

The S&D saturation index (S&DSI) and the saturation of $CaSO_4$ were calculated with ROSA6.1 software [19].

3. Results and discussion

3.1. Results of the first stage

3.1.1. Influence of pressure

The effects of feed pressure on the ions and TDS rejections, as well as the permeate flux, in the first stage are shown in Figs. 2–4. Similar to the normal NF
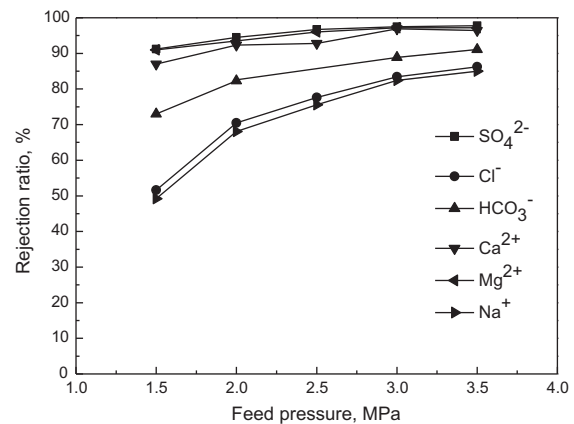
process, the rejection of divalent ions was higher than that of monovalent ions in the seawater system, as shown in Fig. 2. Due to the properties of NF90, the rejection rates of all ions were higher than 50%, and the rejections of SO_4^{2-}, Ca^{2+} and Mg^{2+} could be as high as 90%. The highest TDS rejection was 85%, and the TDS in permeate was 4,500 mg/L, as reported in Fig. 4. Both the permeate flux and ion and the TDS rejections were increased with operating pressure due to the higher driving force. The water permeate flux had a nearly linear relationship with the pressure (see Fig. 3) similar to that in a normal NF and RO process, and the recovery could reach nearly 12% at 3.5 MPa. These results indicated that a large part of seawater TDS could be rejected by NF90 in the first stage, ensuring the quality of water production. The recovery ratio (12%) of a membrane module was also high for a membrane system.
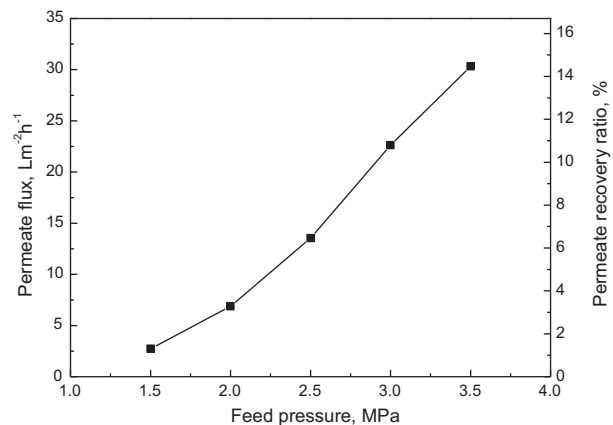

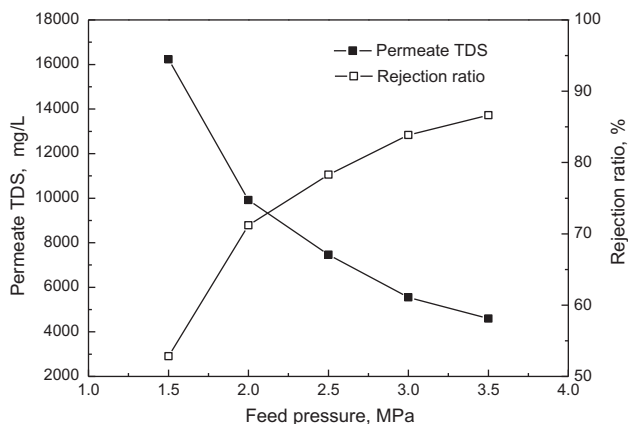Fig. 3. Influence of feed pressure on the permeate flux and permeate recovery ratio ($24°C$, $1.8\,m^3/h$).

Fig. 4. Influence of feed pressure on TDS rejection ratio (24°C, 1.8 m³/h).

3.1.2. Influence of flow rate

The influences of flow rate on the NF performance are demonstrated in Figs. 5–7. It was indicated that both of the ions rejection ratio and permeate flux were increased with the flow rate while the recovery ratio was decreased. The hydrodynamic condition near membrane surface was greatly affected by flow rate, which could be described as follows:

$$K = f(v, D, \text{configuration of module})$$

The mass transfer coefficient (K) is a function of the feed flow velocity (v), diffusion coefficient of the solute (D), viscosity, density, and module configuration [20]. The value of K increased with the feed flow rate (v). Thus, a larger permeate flux was induced by both of these factors. However, the recovery ratio
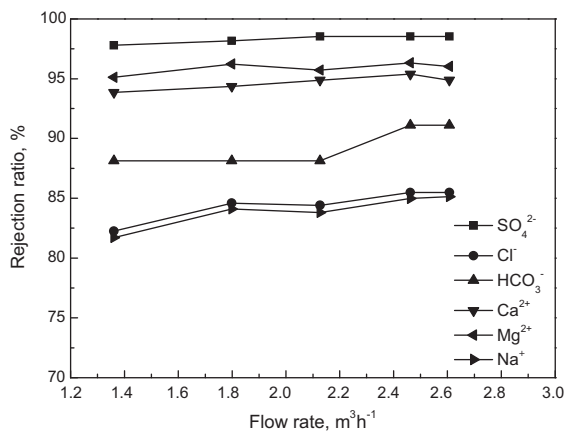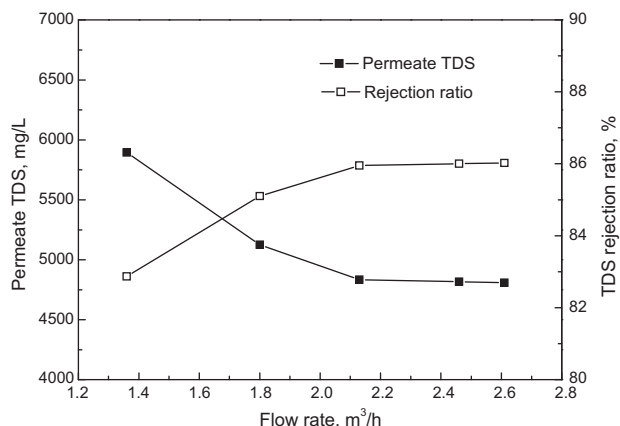

Fig. 6. Influence of feed flow rate on TDS in permeate and TDS rejection ratio (3.5 MPa, 24°C).

(Permeate flux/Feed flow rate) was decreased (see Fig. 5) because the enlargement of the permeate flux feed was small when compared with that of the flow rate. In this experiment, the recovery varied from 13.5 to 7%, whereas the TDS rejection varied from 86 to 83%. The effects of the flow rate were much smaller than that of pressure because the flow rate affected the permeate performance through hydrodynamics.

3.1.3. Influence of temperature

Temperature can influence the membrane permeate properties by affecting the polymer separation layer and the diffusion of ions and water. The polymer chain in the separation layer would swell and be more active under high temperature, which could induce an increase of the membrane pore size. At the same time, the diffusion of ions and water was also

Fig. 5. Influence of feed flow rate on ion rejection ratio (3.5 MPa, 24°C).
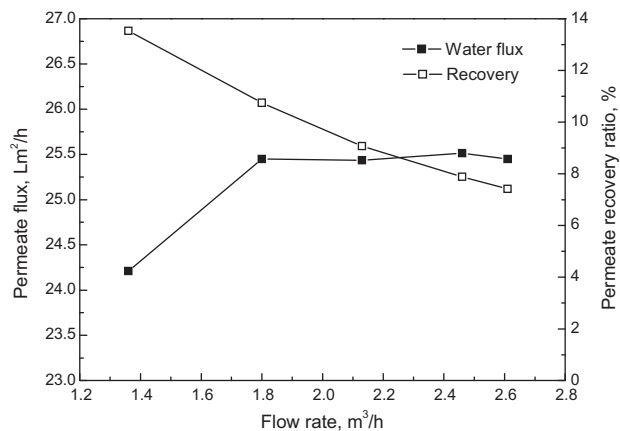

Fig. 7. Influence of feed flow rate on the permeate flux and permeate recovery ratio (3.5 MPa, 24°C).

enhanced under high temperature. Under the combined action of the aforementioned factors, the permeate flux increased with increasing temperature. As shown in Fig. 8, the water permeate flux was also increased with the temperature. Ion rejection was determined by both water permeate flux and ion flux. The results of ions rejection (see Fig. 9) indicated that the effect of temperature on ions rejection was not significant and that the rejection rate of Na^+ and Cl^- slightly decreased, unlike the case of other ions. The latter can be attributed to the smaller modular sizes of Na^+ and Cl^- compared with the other ions, so that these two elements easily permeated the NF membrane and were more sensitive to the temperature. TDS rejection also decreased with temperature, as shown in Fig. 10. These results suggested that a higher temperature is beneficial for large permeate water recovery and increased the permeate TDS. Thus, the controlling of temperature, especially in winter, should be considered.

3.2. Results of the second stage

The results obtained in the first stage indicated that the higher TDS rejection and water permeate flux were induced by the higher feed water pressure and flow rate. Thus, the permeate from the first stage under 3.5 MPa, 2.61 m^3/h and 20°C was selected as the feed water in the second stage. In an industrial process, 6–8 elements are connected end to end in a pressure vessel, and the permeate water from the pressure vessel actually came from the permeate water of each element. However, the TDS difference between each stream was ignored in this paper to facilitate the evaluation. Thus, the permeate water of first stage investigated in Section 3.1. was used as the feed water.
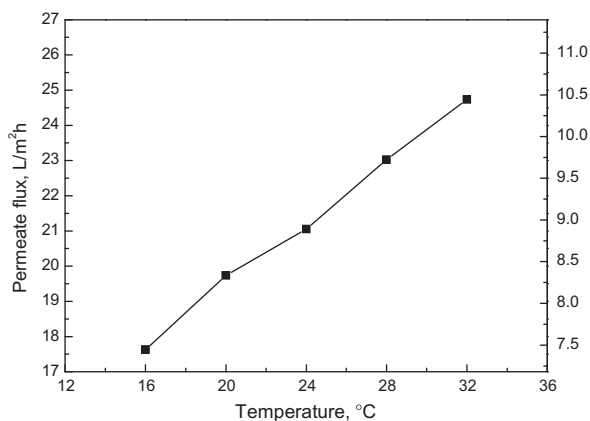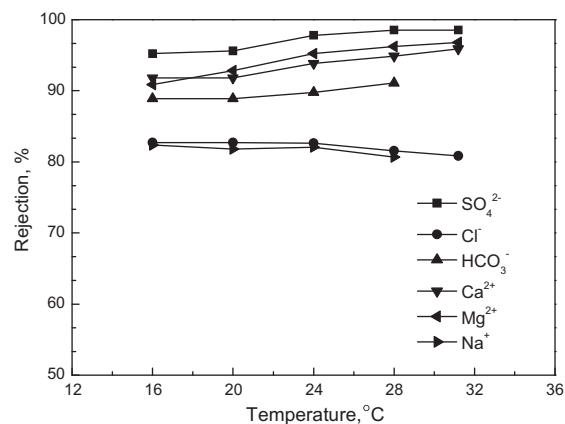
Fig. 9. Effect of feed water temperature on ion rejection ratio (1.8 m^3/h, 3.5 MPa).

The composition is shown in Table 3. The experiment results are reported in Figs. 11–13. The concentrations of Ca^{2+}, Mg^{2+}, HCO_3^-, and SO_4^{2-} in the second stage NF permeate were extremely low (i.e. only approximately several mg/L or even less than 1 mg/L); therefore, the concentration of these ions were not tested and only the TDS was investigated in this experiment.

The effects of pressure, flow rate and temperature during the second stage were similar to the results of first stage, except for the relationship between pressure and permeate TDS. A U-shaped curve was obtained in the study of relationship of TDS with pressure; in this relationship, the lowest TDS existed, which can be attributed to the higher water permeate flux in the second stage. The permeate TDS could be presented as $C_p = J_s/J_w$ in the membrane process, so that the value could be affected not only by solute permeate flux, but also by the water permeate flux. Water permeate flux was considerably higher in the
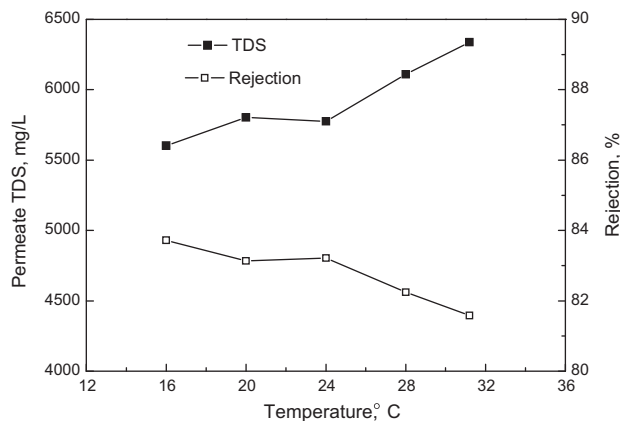
Fig. 8. Effect of temperature on water flux and recovery (1.8 m^3/h, 3.5 MPa).

Fig. 10. Effect of feed temperature on permeate TDS and TDS rejection ratio (1.8 m^3/h, 3.5 MPa).

Table 3
Ions concentration in feed water of second stage

Ion	Concentration mg/L
SO_4^{2-}	120
HCO_3^-	14
Cl^-	2,910
Ca^{2+}	20
Mg^{2+}	80
Na^+	1,780
TDS	4,924

second stage; therefore, a more severe concentration polarization phenomenon was induced under high operating pressure. The permeation of solute ions was increased rapidly due to increase in the trans-membrane concentration difference; whereas, the growth of permeate water flux decelerated because of the increase of osmotic pressure. The TDS in permeate water increased slightly under higher operating pressure, under the combined action of the two aforementioned factors. The permeate TDS, after the second stage, could be lower than 250 mg/L in a variety of operating conditions, and the lowest value could reach 190 mg/L. Thus, the dual-stage NF seawater desalination is technically feasible in producing fresh water that meets the quality standards for drinking water.

3.3. Influence of operating condition on the membrane scaling possibility

The S&DSI and the saturation of retentate $CaSO_4$ (S_{CaSO_4}) were calculated with ROSA 6.1 software to investigate the possibility of membrane scaling. The concentration of the retentate stream was calculated, based on the single-element experiment results presented in Sections 3.1. and 3.2. Six elements in one pressure vessel were supposed to be of use in both the first and second stages. The recovery ratio was calculated from each element as following:

$$F_i = F_{i-1} \cdot \left(\frac{1 - R_{i-1}}{R_{i-1}} \right) \cdot R_i \qquad (2)$$

$$R_s = \frac{\sum_{i=1}^{6} F_i}{F_0} \qquad (3)$$

where F_i is the permeate flow rate of element i, R_i is the recovery ratio of element i, F_0 is the feed water flux of pressure vessel, and R_s is the recovery ratio of whole pressure vessel. To simplify the calculation process, the value of R_i was assumed to be same as the one in Sections 3.1. and 3.2., and the ion concentrations in retentate were calculated. The results in Figs. 14–16 indicated that both S&DSI and saturation were increased, following the operating pressure and temperature, which were decreased with the flow rate shown in Fig. 15. Among these three factors, pressure had the most evident effect on the scaling index primarily because the permeate flux and TDS rejection was greatly affected by the feed pressure. Thus, the ion concentrations were influenced, whereas the influences of temperature and flow rate were smaller. Meanwhile, the S&DSI and saturation in the first stage were considerably greater than that in second stage due to the higher concentration of feed water. All of S&DSI values were positive in the first stage, which indicated that the scaling of calcium carbonate could easily occur in the retentate stream. Thus, adjustment
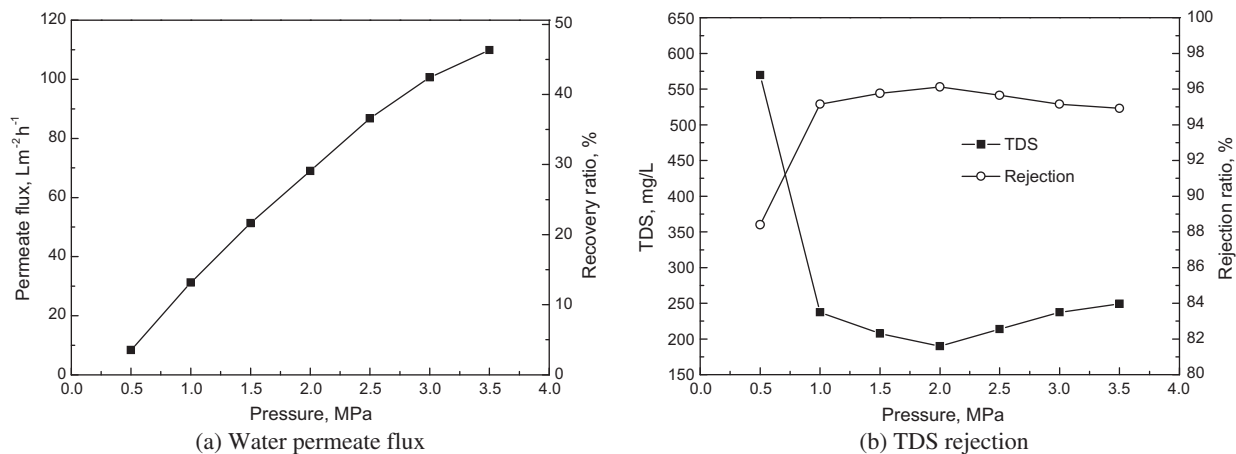

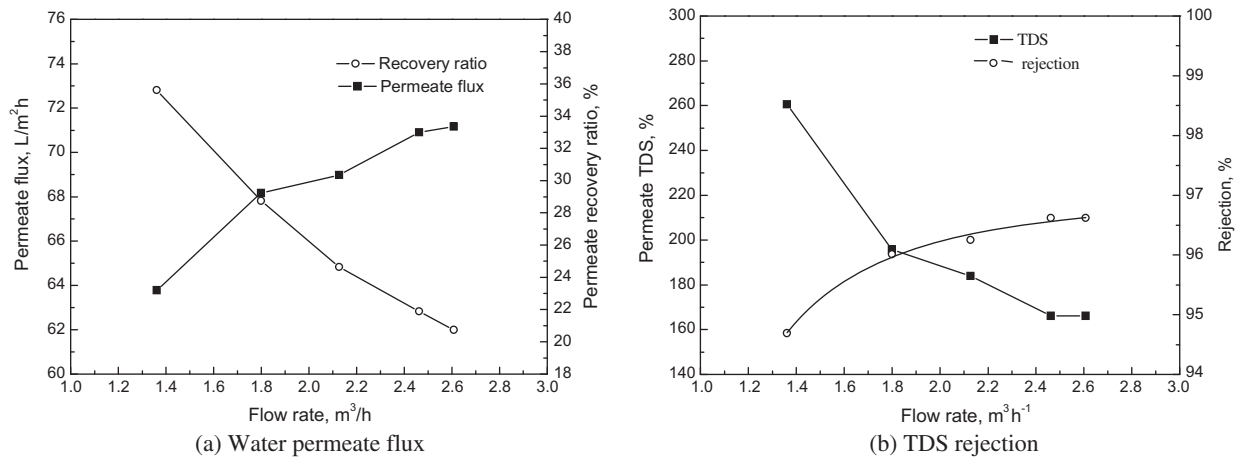Fig. 11. Influence of feed pressure on membrane performance (1.8 m³/h, 20°C).

(a) Water permeate flux

(b) TDS rejection

Fig. 12. Influence of feed flow rate on membrane performance (2.0 MPa, 20°C).

(a) Water permeate flux

(b) TDS rejection
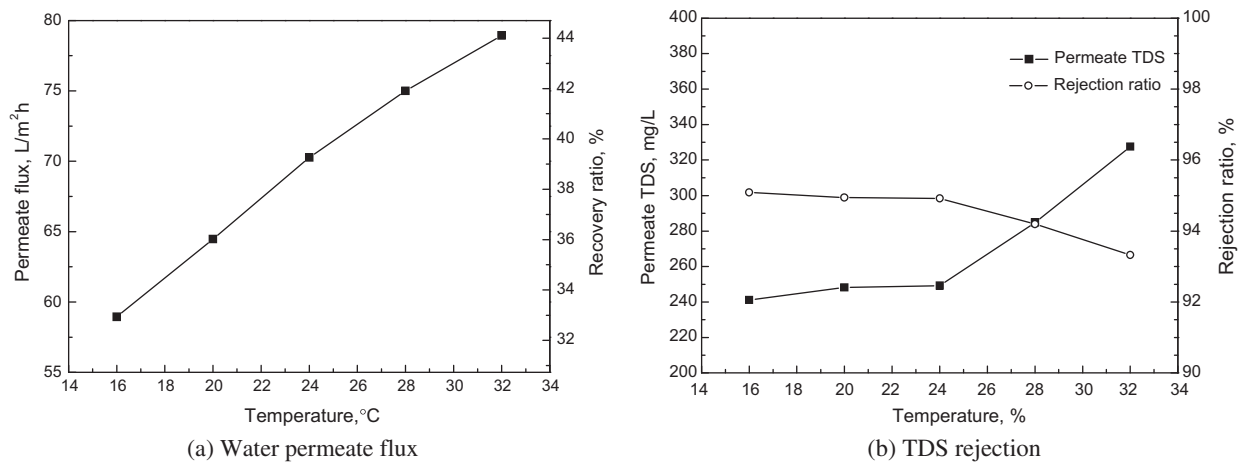
Fig. 13. Effect of temperature on the membrane performance (1.36 m^3/h, 2.0 MPa).

(a) Influence of feed pressure on S&DSI

(b) Influence of feed pressure on St$_{CaSO4}$
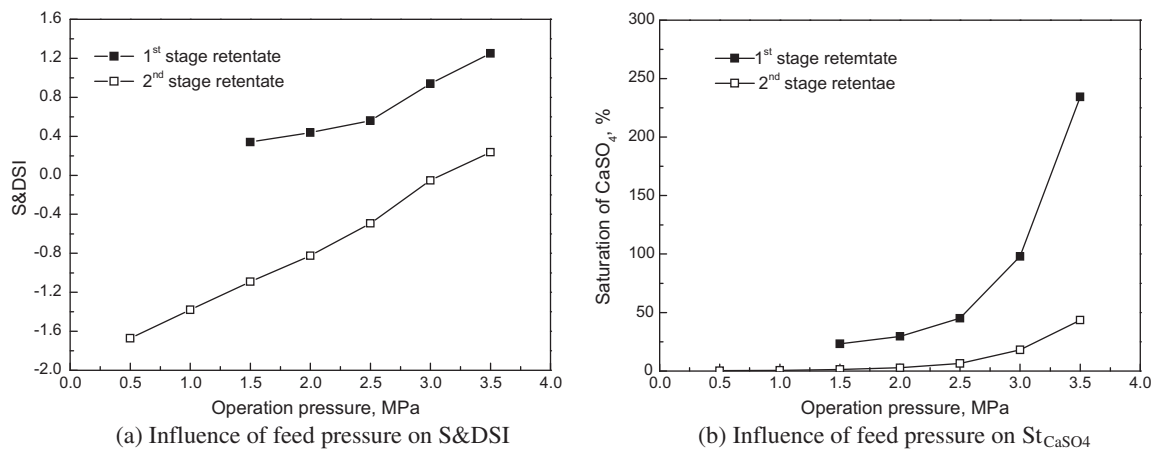
Fig. 14. S&DSI and saturation of retentate CaSO$_4$ under different feed pressure.

(a) Influence of flow rate on S&DSI

(b) Influence of flow rate on S_{CaSO4}
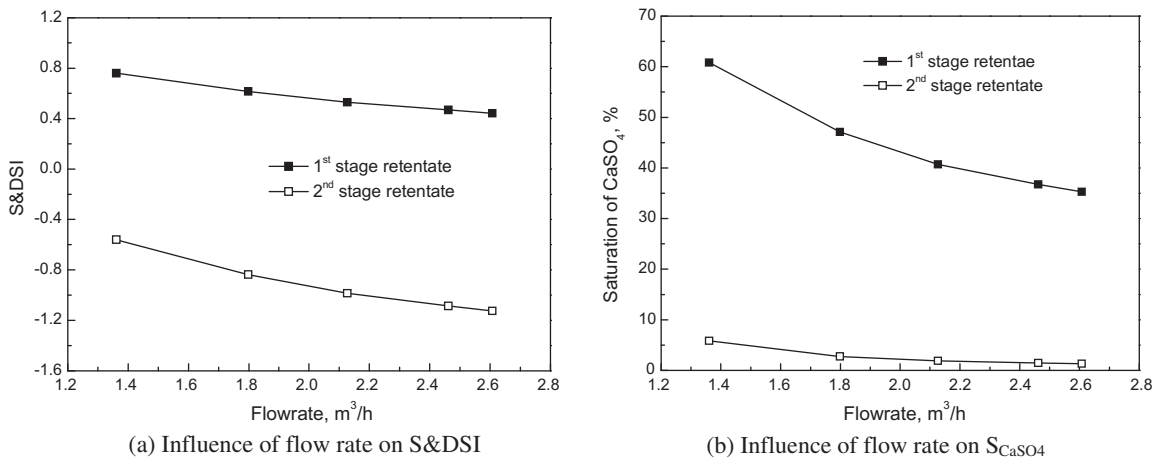
Fig. 15. S&DSI and saturation of retentate $CaSO_4$ under different flow rate.

(a) Influence of temperature on S&DSI

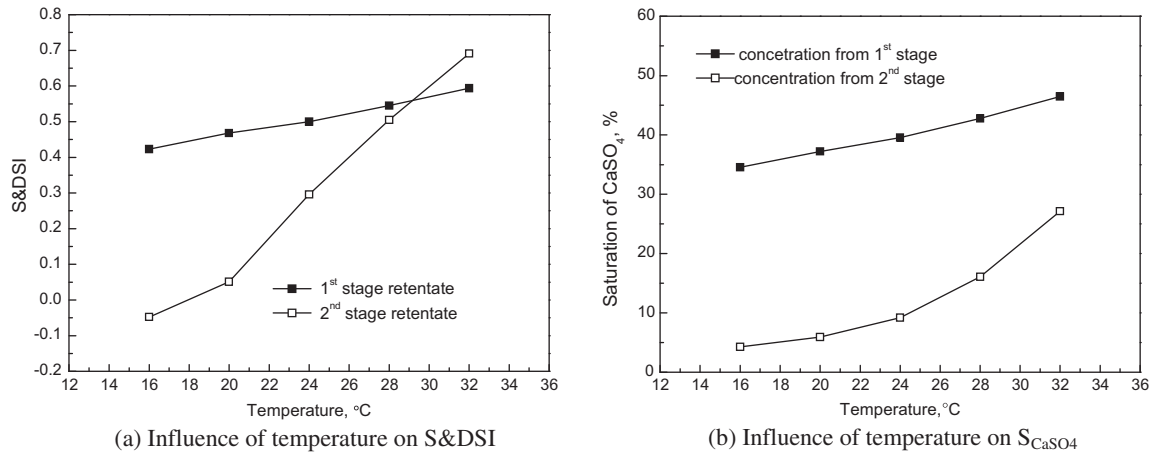(b) Influence of temperature on S_{CaSO4}

Fig. 16. S&DSI and saturation of retentate $CaSO_4$ under different temperature.

of pH or a scale inhibitor was needed in the first stage to prevent membrane scaling. Most of the scaling ions were removed in the first stage; therefore, the two indices were significantly lower in the second stage. Most of the S&DSI values were negative, except the one under high operating pressure and temperature, from which a higher recovery ratio could be obtained. These results indicated that the scaling prevention method was essential in the first stage, which was not necessary in second stage when appropriate recovery ratio was selected.

From the results of the permeate water flux and TDS, it was shown that scaling would occur along with the high recovery ratio and TDS rejection level. Thus, the optimization of operating conditions should consider all of these aspects.

3.4. Effect of operating condition on energy consumption

The diagram of the single-stage seawater desalination process is shown in Fig. 17, where P is the pressure (MPa) and F is the flow rate (m³/h). The effective power supplied by the boost pump could be calculated by:

$$W = \frac{1}{3.6}(P_2 - P_1) \times F_1 \qquad (4)$$

where W is the effective power, kW. Thus, the specific energy consumption can be calculated by the following formula:

$$Q = \frac{W}{\eta F} = \frac{(P_2 - P_1) \times F_1}{\eta F_3} = (P_2 - P_1)\frac{1}{3.6\eta R_s} \qquad (5)$$
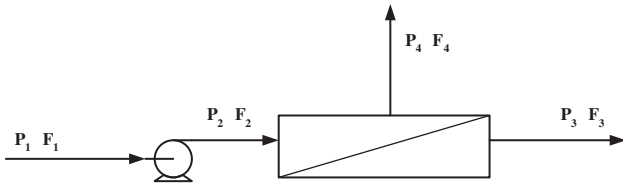
Fig. 17. Diagram of single stage seawater desalination process.

where Q is the specific energy consumption per m^3 permeate water, kWh/m^3, and η is the energy efficiency, <1. Except for η, the other parts are defined as energy coefficient A:

$$A = \frac{(P_2 - P_1)}{3.6 R_s} \tag{6}$$

where R_s is the system recovery:

$$R_s = \frac{F_3}{F_2} = \frac{F_3}{F_1} \tag{7}$$

The overall energy consumption of dual-stage NF seawater desalination could be calculated as:

$$Q_s = \frac{R_1 Q_1 + R_1 R_2 Q_2}{R_1 R_2} = \frac{1}{R_2} Q_1 + Q_2 \tag{8}$$

When η is assumed to be same in each stage, the overall energy coefficient A_s could be represented as:

$$A_s = \frac{1}{R_2} A_1 + A_2 \tag{9}$$

where the subscript 1 and 2 is the corresponding value in first and second stage. The energy coefficient A is associated with the operating conditions, and η is affected by the efficiency of the pump and motor and by the pressure loss in the pipe. Thus, the effect of operating condition on energy consumption was investigated by identifying the variations of A. The system recovery ratio R_s was calculated in the dual-stage process by following Eqs. (2) and (3), in which each stage comprised one pressure vessel containing six elements. The basic data was obtained from the results of Sections 3.1. and 3.2.

The calculated results are reported in Figs. 18–20. As shown in the figures, the energy consumption coefficients (A) decreased with operating pressure, but temperature increased with feed-water flow rate. All of these results were determined by the ratio of operating pressure to recovery, as shown in Eq. (4). When the operating pressure was kept constant, flow rate and temperature had the opposite effect on the system recovery ratio, which increased with temperature and decreased with flow rate; therefore, the value of A also differed. The effect of operating pressure was slightly complicated. Water permeate flux increased with operating pressure; however, the concentration polarization near membrane surface would be more severe under high pressure. Thus, the growth of water flux decelerated under high pressure, as illustrated in Figs. 3 and 11(a). The decelerated growth of the water flux facilitated a slow decrease in energy consumption and tended to remain constant. Among these three factors (pressure, temperature and flow rate), the effects of pressure on the energy consumption was most prominent, whereas the influence of temperature
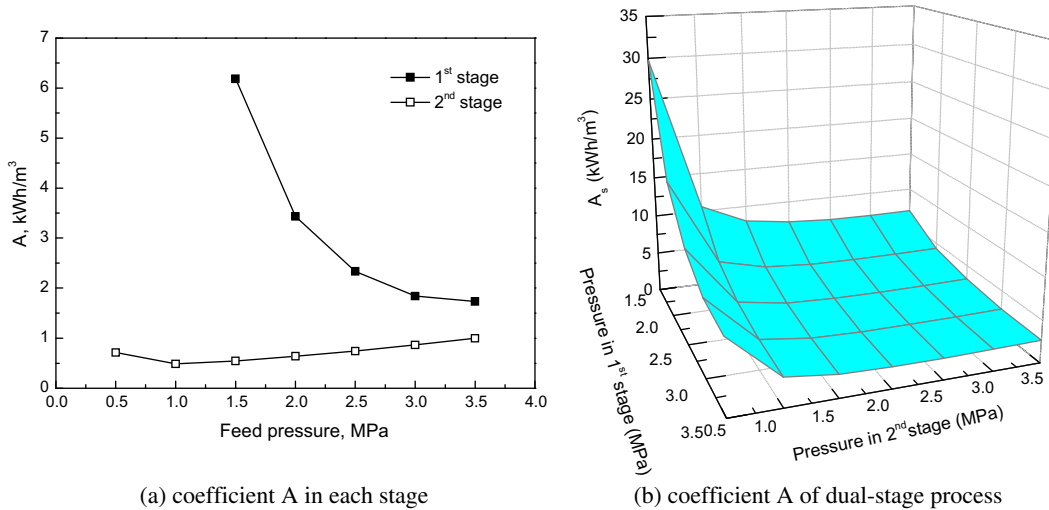

(a) coefficient A in each stage

(b) coefficient A of dual-stage process

Fig. 18. Effect of pressure on the energy consumption coefficient A (first stage: 8 cm/s, 20°C and second stage: 8 cm/s, 20°C).

(a) coefficient A in each stage
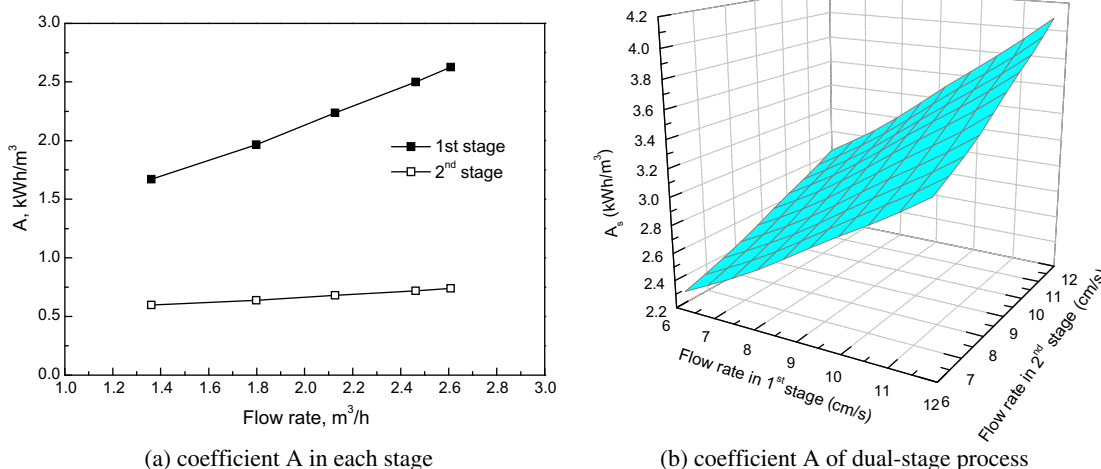

(b) coefficient A of dual-stage process

Fig. 19. Effect of flow rate on energy consumption coefficient A (first stage: 3.5 MPa, 20°C and second stage: 2.0 MPa, 20°C).
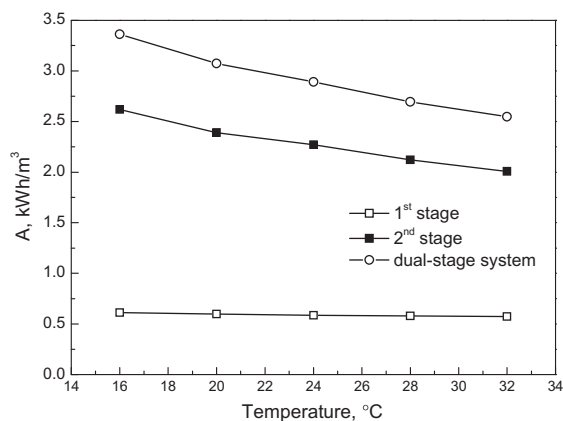

Fig. 20. Effect of temperature on energy consumption coefficient A (first stage: 8 cm/s, 3.5 MPa; and second stage: 6 cm/s, 2.0 MPa).

was least prominent. The coefficients A of dual-stage system were also shown in Figs. 18(b), 19(b), 20. It was indicated that first stage has a notable effect on the A_s due to its large energy consumption, which could also be seen in Eq. (9).

Unlike operating pressure, the system recovery ratio decreased with the increase in flow rate in both the first and second stages, as shown in Figs. 5 and 12. Thus, the energy consumption increased. The inference can be made that operation under a higher flow rate is not energy-saving; but turbulence near the membrane surface could be enhanced, so that the scaling possibility could still be reduced.

4. Conclusions

Single-element equipment was set up to simulate the dual-stage NF seawater desalination process. The effects of operating pressure, temperature, and flow rate on the ions and TDS rejection, permeation flux, and the index of scaling possibility, respectively, were investigated. The primary conclusions of the study can be summarized as follows:

- The ions and TDS rejections, as well as permeate water flux, were evidently influenced by operating pressure. The effect of feed-flow rate and temperature were less significant than that of pressure. The TDS in permeate water after the second stage could be as low as 200 mg/L, which would meet the quality standards for drinking water.
- The operating conditions (feed pressure, flow rate and temperature) had a significant effect on the membrane scaling. A scaling possibility was observed in the first stage; therefore, pH adjustment or a scale inhibitor was needed. Langelier saturation index (LSI) and S_{CaSO_4} were lower in the second stage because most of the scaling ions were rejected in first stage and the concentration decreased in second stage.
- Energy consumption was greatly influenced by feed pressure and the recovery ratio. Operating pressure had the most evident effect among the three factors. Energy consumption in the first stage was considerably greater than that in the second stage. Thus, the energy consumption in the first stage had to be decreased by optimizing the operating parameters, or by using an energy recovery device.

The results of this study indicated that dual-stage NF seawater desalination is a feasible technology. The scaling possibility in the first stage should be considered. The recovery ratio, TDS rejection, scaling and energy consumption should likewise be considered in the practical desalination process.

Symbols

TDS	—	total dissolved solids, mg/L
RO	—	reverse osmosis
MSF	—	multi-stage flash
MED	—	multi-effect distillation
NF	—	nanofiltration
BWRO	—	brackish water reverse osmosis
S&DSI	—	Steven and David saturation index
LSI	—	Langelier saturation index
IP_{CaSO_4}	—	ions product of $CaSO_4$
K	—	mass transfer coefficient
v	—	flow velocity, m/s
D	—	diffusion coefficient
C_p	—	ions concentration in permeate, mg/L
J_s and J_w	—	permeate flux(solute & water), g/s
P	—	pressure, MPa
F	—	flow rate, m^3/h
W	—	effective power, kW
Q	—	specific energy consumption, kWh/m^3
η	—	energy efficiency, %
A	—	energy coefficient, kWh/m^3
R	—	system recovery, %

References

[1] Akili D. Khawaji, Ibrahim K. Kutubkhanah, Jong-Mihn Wie, Advances in seawater desalination technologies, Desalination 221(1–3) (2008) 47–69.

[2] H. Ludwig, Energy Consumption of Seawater Reverse Osmosis: Expectations and Reality for State-of-the-Art Technology, IDA World Congress, Dubai, UAE, 2009.

[3] R.L. Stover, Evolution of energy consumption in seawater reverse osmosis, Desalination and Water Reuse 19(2) (2009) 27–30.

[4] International Desalination Association, IDA Desalination, Year Book 2009–2010, pp. 1–7.

[5] Franz Trieb, Hans Müller-Steinhagen, Jürgen Kern et al., Technologies for large scale seawater desalination using concentrated solar radiation, Desalination 235(1–3) (2009) 33–43.

[6] H.M. Lu, J.C. Walton, A.H.P. Swift, Desalination coupled with salinity-gradient solar ponds, Desalination 136(1–3) (2001) 13–23.

[7] Shaobo Hou, Hefei Zhang, A hybrid solar desalination process of the multi-effect humidification dehumidification and basin-type unit, Desalination 220(1–3) (2008) 552–557.

[8] E. Mathioulakis, V. Belessiotis, E. Delyannis, Desalination by using alternative energy: Review and state-of-the-art, Desalination 203(1–3) (2007) 346–365.

[9] B.M. Hamieh, J.R. Beckman, Seawater desalination using Dew vaporation technique: Theoretical development and design evolution, Desalination 195(1–3) (2006) 1–13.

[10] Jean-Pierre Mericq, Stéphanie Laborie, Corinne Cabassud, Evaluation of systems coupling vacuum membrane distillation and solar energy for seawater desalination, Chemical Engineering Journal 166(1–3) (2011) 596–606.

[11] B.M. Hamieh, J.R. Beckman, Seawater desalination using Dew vaporation technique: Experimental and enhancement work with economic analysis, Desalination 195(1–3) (2006) 14–25.

[12] Yuefei Song, Jia Xu, Yan Xu et al., Performance of UF–NF integrated membrane process for seawater softening, Desalination 276(1–3) (2011) 109–116.

[13] Ahmed S. Al-Amoudi, A. Farooque, Performance restoration and autopsy of NF membranes used in seawater pretreatment, Desalination 178 (1–3) (2005) 261–271 (SPEC. ISS.).

[14] Song, Yuefei, Su, Baowei, Gao, Xueli, Gao, Congjie, The performance of polyamide nanofiltration membrane for long-term operation in an integrated membrane seawater pretreatment system, Desalination 296 (1–3) (2012) 30–36.

[15] Osman A. Hamed, Overview of hybrid desalination systems – current status and future prospects, Desalination 186 (1–3) (2005) 207–214.

[16] C.J. Harrison, Y.A. Le Gouellec, R.C. Cheng et al., Bench-scale testing of nanofiltration for seawater desalination, Journal of Environmental Engineering 133(11) (2007) 1004–1014.

[17] R.C. Chen, D.X. Vuong et al., The use of dual-staged nanofiltration menbranes for seawater desalination, desalination of seawater and brackish water, American Water Works Association 67–77.

[18] Ali AlTaee, Adel O. Sharif, Alternative design to dual stage NF seawater desalination using high rejection brackish water membranes, Desalination 273(1–3) (2011) 391–397.

[19] http://www.dow.com/liquidseps/design/rosa.htm.

[20] Marcel Mulder, Basic Principles of Membrane Technology, second ed., Kluwer Academic Publisher, Netherlands, pp. 418–424.